

Rigid-Band Shift of the Fermi Level in a Strongly Correlated Metal: $\text{Sr}_{2-y}\text{La}_y\text{RuO}_4$

N. Kikugawa,^{1,2,3} A.P. Mackenzie,¹ C. Bergemann,⁴ R.A. Borzi,¹ S.A. Grigera,¹ and Y. Maeno^{3,5}

¹*School of Physics and Astronomy, University of St. Andrews, St. Andrews Fife KY16 9SS, United Kingdom*

²*Venture Business Laboratory, Kyoto University, Kyoto 606-8501, Japan*

³*Department of Physics, Kyoto University, Kyoto 606-8502, Japan*

⁴*Cavendish Laboratory, University of Cambridge,*

Madingley Road, Cambridge CB3 0HE, United Kingdom

⁵*International Innovation Center, Kyoto University, Kyoto 606-8501, Japan*

(Dated: July 11, 2018)

We report a systematic study of electron doping of Sr_2RuO_4 by non-isovalent substitution of La^{3+} for Sr^{2+} . Using a combination of de Haas-van Alphen oscillations, specific heat, and resistivity measurements, we show that electron doping leads to a rigid-band shift of the Fermi level corresponding to one doped electron per La ion, with constant many-body quasiparticle mass enhancement over the band mass. The susceptibility spectrum is substantially altered and enhanced by the doping but this has surprisingly little effect on the strength of the unconventional superconducting pairing.

PACS numbers: 74.70.Pq, 74.62.Dh, 74.25.Jb

The layered perovskite transition-metal-oxide Sr_2RuO_4 has been the subject of intensive research over the past decade. In its stoichiometric form, it can be grown with very high purity, allowing the observation of what is now known to be an unconventional, probably spin-triplet, superconducting state at low temperatures [1, 2, 3]. Extensive de Haas-van Alphen (dHvA) studies have revealed precise information about its Fermi-surface topography with three nearly cylindrical sheets based on bands with combined Ru d and oxygen p character: one hole sheet (α) and two electron sheets (β and γ) [4, 5, 6, 7, 8, 9]. The dynamical susceptibility has features both at the wave vector $\mathbf{q} \sim (2\pi/3, 2\pi/3, 0)$ [10], and around $\mathbf{q} \sim 0$ [6, 11], both of which can be accounted for in terms of the known Fermi surfaces [5, 12, 13].

In contrast to the unusually depth understanding of the normal metallic state, far less is known about the superconducting mechanism. While our experimental and phenomenological knowledge of the superconductivity of pure Sr_2RuO_4 is exhaustive [3], it still provides insufficient constraints for models for the microscopic pairing mechanism. Here, the most common assumption is that the dominant sheet is γ , since it has the largest mass-enhancement and low- q susceptibility [14]. One method for obtaining additional and complementary information on correlated electron systems is chemical doping, a technique that has been widely applied in recent years [15]. This has motivated studies of Sr_2RuO_4 in which the Ru has been doped with Ti [16, 17, 18, 19] and Ir [20], and the Sr substituted by Ca [21], focusing on the magnetic properties in each system. Each of these has revealed rich new physics, but with the commonly-experienced complication of introducing strong potential scattering and structural distortion.

In this paper, we concentrate on non-isovalent counterion substitution of Sr^{2+} with La^{3+} . In contrast to isovalent Ca-doping, the primary effect of La doping is the introduction of extra electrons to the metallic bands at the Fermi energy. At the same time, the main

electronic “building blocks”—the RuO_2 planes—remain structurally unaffected, unlike the previously studied case of Ti/Ir substitution. Also, since the ionic radii of Sr^{2+} and La^{3+} are very similar, structural distortions are minimized. La substitution therefore provides a gentle way to study electron doping and the effect of changing carrier concentration in the correlated metal and unconventional superconductor Sr_2RuO_4 .

We present here the results of a combined dHvA, resistivity, specific heat, and magnetic susceptibility study on samples of $\text{Sr}_{2-y}\text{La}_y\text{RuO}_4$ extending up to $y = 0.10$. It is remarkable in itself that the dHvA effect is observable, and we are able to show in detail that the normal state undergoes a rigid shift of the Fermi level with unchanged correlation quasiparticle mass enhancement: an unexpected result for this multi-band, correlated metal [22], especially considering the vicinity of the van Hove singularity associated with the γ band. Although the absolute quasiparticle masses and the spin susceptibility spectrum are strongly affected by carrier doping, the evolution of the superconducting transition temperature T_c indicates no change in pairing strength, which introduces new and strong constraints on candidate pairing mechanisms.

Single crystals of $\text{Sr}_{2-y}\text{La}_y\text{RuO}_4$ with y up to 0.10 were grown by a floating-zone method [23] with an infrared image furnace (NEC Machinery, model SC-E15HD) at Kyoto University. The La concentrations were determined by electron-probe microanalysis (EPMA). Tetragonal symmetry was confirmed for all crystals by x-ray powder diffraction measurements at room temperature. The lattice parameter along the in-plane direction increases by $\sim 0.2\%$ and that perpendicular to the plane decreases by $\sim 0.15\%$ continuously up to $y = 0.10$.

The dHvA experiments were performed at the University of St. Andrews by a field modulation technique [24] at temperatures down to 40 mK, with the magnetic field applied along the c axis with an accuracy of better than 3° . The in-plane resistivity ρ_{ab} was measured by a

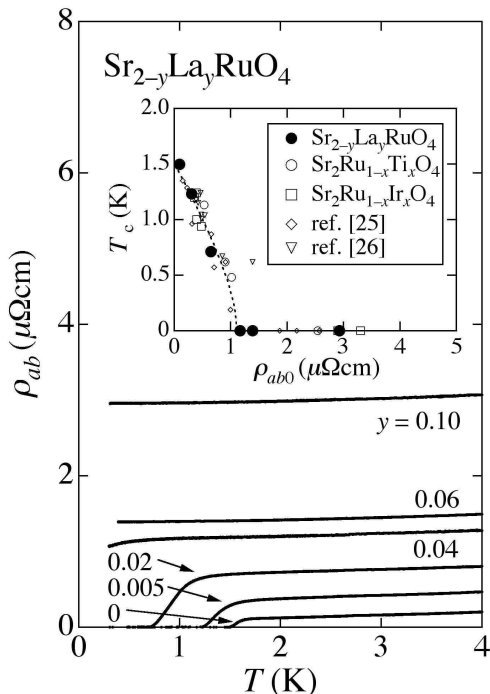


FIG. 1: Temperature dependence of the ρ_{ab} in $\text{Sr}_{2-y}\text{La}_y\text{RuO}_4$ with y up to 0.10. Inset: The T_c as a function of the in-plane residual resistivity ρ_{ab0} for $\text{Sr}_{2-y}\text{La}_y\text{RuO}_4$. Previous results for different sources of disorder are also shown. The broken line shows the Abrikosov-Gor'kov pair-breaking function.

low frequency ac method between 0.3 and 5 K. Magnetic susceptibility measurements were performed using a superconducting quantum interference device magnetometer (Quantum Design, MPMS-XL). The specific heat C_P was measured by a thermal relaxation method from 0.5 K and 30 K (Quantum Design, model PPMS).

Figure 1 shows the temperature dependence of ρ_{ab} in $\text{Sr}_{2-y}\text{La}_y\text{RuO}_4$ up to $y=0.10$. The superconducting transition temperature T_c is gradually and systematically suppressed with an initial rate $dT_c/dy \sim -40$ K/ y ; it reaches zero at $y \sim 0.03$. As shown in the inset of Fig. 1, the suppression of T_c is well scaled by the Abrikosov-Gor'kov pair-breaking function for unconventional superconductivity. The most striking feature of the inset is that the data are seen to follow a universal curve if plotted as a function of the residual resistivity ρ_{ab0} (defined by extrapolating the normal state ρ_{ab} to $T=0$). T_c is completely suppressed at $\rho_{ab0} \sim 1.1 \mu\Omega\text{cm}$; this value and the form of the $T_c(\rho_{ab0})$ curve are identical for La and various other kinds of impurities and defects [18, 20, 25, 26].

The rate at which the La dopants between the RuO_2 planes introduce scattering is, as expected for an out-of-plane dopant, much smaller than that for in-plane substituted impurities such as Ti and Ir for Ru [18, 20]. The residual resistivity, ρ_{ab0} , increases systematically with y at the rate of $d\rho_{ab0}/dy \sim 40 \mu\Omega\text{cm}/y$, that is, with a

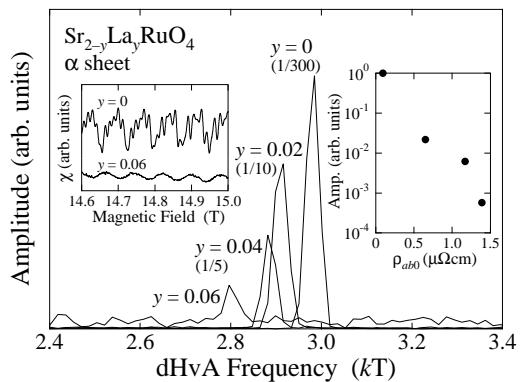


FIG. 2: The dHvA frequency spectrum for the α sheet of $\text{Sr}_{2-y}\text{La}_y\text{RuO}_4$ up to $y=0.06$. The left inset shows quantum oscillatory susceptibility χ of $\text{Sr}_{2-y}\text{La}_y\text{RuO}_4$ with $y=0$ and 0.06. The dependence of the dHvA amplitude on the in-plane residual resistivity ρ_{ab0} is presented in the right inset. Note the logarithmic scale on the vertical axis.

phase shift for impurity scattering $\delta_0 \sim \pi/12$. In contrast, Ti and Ir act as unitary scatterers with $\delta_0 \sim \pi/2$ [20]. However, we reiterate that although the rate at which the La ions affect the resistivity is lower than for Ti or Ir, the effect of that change of resistivity on the superconductivity is independent of the dopant species.

Fig. 2 shows the Fourier transform of the dHvA oscillations for $\text{Sr}_{2-y}\text{La}_y\text{RuO}_4$ up to $y=0.06$, in a narrow frequency region around the α branch. Sample oscillations are shown in the left inset of Fig. 2 for $y=0$ and 0.06. For pure Sr_2RuO_4 with $T_c=1.44$ K, not only the whole frequency spectrum with three Fermi-surface sheets but also additional harmonics α and linear combinations such as $\alpha + \beta$ are detected. The oscillatory amplitude is exponentially suppressed by La substitution, reflecting the introduction of weak disorder, as seen in the right inset in Fig. 2. The effect is strongest on the large γ sheet so that even at $y=0.02$ ($\rho_{ab0} \sim 0.7 \mu\Omega\text{cm}$) its signal is unobservable. For $y=0.06$, only the α frequency remains detectable (left inset of Fig. 2), and no oscillations at all are found for $y=0.10$ in our current study.

The exponential decay of the signal with doping gives the opportunity for a reliable Dingle analysis. The suppression factor is $\exp(-\pi r_c/\ell)$, where r_c is the cyclotron radius and ℓ is the carrier mean free path. The values obtained for the α sheet range from 990 ± 100 nm for $y=0$ to 76 ± 9 nm for $y=0.06$. These agree, within the stated error, with the values obtained by an analysis of the resistivity under the “isotropic mean-free-path approximation” [4, 6]. This is interesting because it implies that the resistivity, which is biased towards large angle scattering, still gives a good estimate of the scattering (including small angle events) that damps the quantum oscillations, even though the out-of-plane La ions act as relatively diffuse scattering centers.

A more significant feature of the data is that we ob-

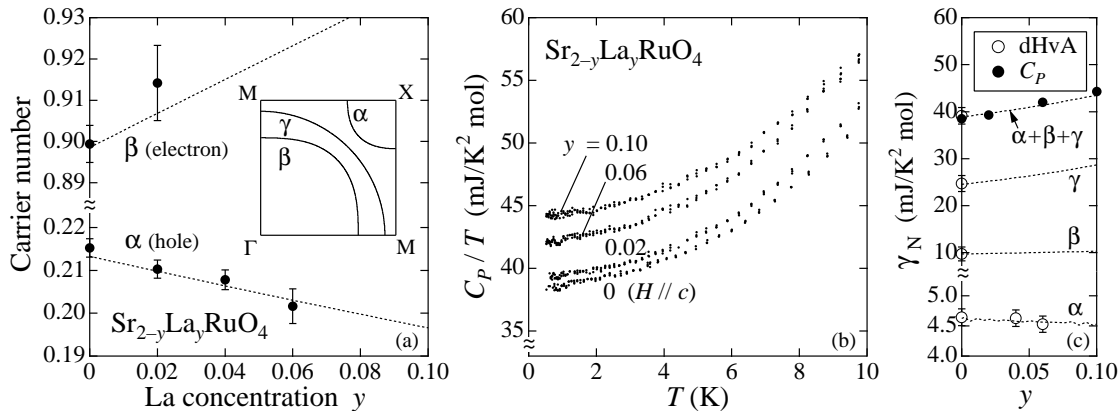


FIG. 3: (a) La concentration dependence of the carrier number of the α and the β sheets. The γ sheet dependence is not shown since we have data only at $y=0$, but it corresponds to an increase of approximately 0.03 electrons by $y=0.06$. Inset: A sketch of the Fermi surface of Sr_2RuO_4 . (b) Temperature dependence of C_P/T in $\text{Sr}_{2-y}\text{La}_y\text{RuO}_4$ up to $y=0.10$. (c) Doping dependence of γ_N (for definition see text). Closed (open) circles represent data from specific heat (dHvA) measurements. The dotted lines show the prediction of the calculation described in the text. The error bars on the dHvA-derived sheet-specific contributions reflect the combined uncertainties of the data and the parameters used in the calculation.

serve progressive changes in the dHvA oscillation frequencies F_{ext} , as shown in Fig. 2. Since these frequencies directly relate to the cross-sectional areas of the Fermi-surface sheets via $A_{\text{ext}} = 2\pi e F_{\text{ext}}/\hbar$, this reflects a change in the carrier concentration associated with each sheet. As seen in Fig. 3(a), the hole-like α sheet shrinks while the electron-like β sheet grows in size, which is completely consistent with the La acting as an electron donor.

A much more quantitative analysis is also possible in this system. The years of work on pure Sr_2RuO_4 have led to the construction of an empirically determined tight-binding model for the electronic structure, derived from fits to the experimentally determined Fermi surface [6]. The dotted lines in Fig. 3 are not fits or guides to the eye, but topography calculations based on this model, without free parameters, under the assumption that each La dopes one free electron and induces a rigid shift of the Fermi level. As can be seen, the agreement is excellent. This is remarkable, because although Luttinger’s theorem usually puts strong enough constraints on the Fermi-surface geometry for such rigid-band shift calculations to work at least approximately in single-band systems, the constraints are much less powerful for a multi-band system such as Sr_2RuO_4 . In Ca-substituted Sr_2RuO_4 , for example, doping lowers the d_{xy} band with respect to the $d_{yz/zx}$ system [21]; similarly, correlations among electrons can influence the evolution of the Fermi-surface geometry, especially in metals with both electron and hole pockets [22]—but in strongly correlated $\text{Sr}_{2-y}\text{La}_y\text{RuO}_4$, both effects are either absent or compensate each other.

We can also use the tight-binding model and its density of states to predict each sheet’s contribution to the specific heat C_P/T as a function of y . The experimental C_P/T is strongly enhanced over the bare density of states by electron-phonon and electron-electron interactions; we empirically set this enhancement to be inde-

pendent of y and use the well-known values for pure Sr_2RuO_4 [6]. In Fig. 3(b), we show the C_P/T as a function of temperature for various values of y . The phonon term has not been extracted, so the electronic contribution, defined as γ_N , is given by the extrapolation to zero temperature (well approximated by the lowest temperature value in each case). These values are plotted against y in Fig. 3(c) (filled circles); that plot also contains the individual sheets’ contributions (open circles) as inferred from analysis of dHvA temperature damping. The dashed lines are the calculations from the tight-binding model, in which the quasiparticle mass-enhancement over the band mass is taken to be constant throughout the doping range, and again, the agreement is excellent: the experimental C_P/T rises with y , and the contribution from the α sheet decreases slightly, in line with the calculation.

The rapidly increasing experimental value for the electronic C_P/T , and the underlying tight-binding model, imply a large change ($> 15\%$) to the γ sheet mass on doping. This is not surprising, since the electron doping is qualitatively expected to shift the Fermi level for that band towards the van Hove singularity [6, 8, 14]. We have observed an even more substantial (30%) change to the low temperature static susceptibility $\chi(q=0)$ (data not shown): the increase in the density of states is augmented here by the feedback mechanism arising from the Stoner factor.

Along with the bulk $\chi(q=0)$, the whole spin-susceptibility spectrum $\chi(\mathbf{q})$ has to change significantly on electron doping. In pure Sr_2RuO_4 , $\chi(\mathbf{q})$ reflects the nesting properties of the Fermi surface [5, 12, 13], with features both at wave vector $\mathbf{q} \sim (2\pi/3, 2\pi/3, 0)$ [10] from α/β nesting, and at low q [6, 11] from the γ sheet [27]. Electron doping will shift the α/β nesting to smaller wave vectors, and enhance the low- q susceptibility as the γ

sheet moves closer to the van Hove singularity.

Many theories attribute the superconducting pairing in Sr_2RuO_4 to spin fluctuations in either the γ or α/β channel, where the more common assumption is that the dominant sheet is γ , since it has the largest mass-enhancement and low- q susceptibility. The relation between the spin-fluctuation spectrum $\chi(\mathbf{q})$ and T_c and ξ is a subtle one and certainly beyond the scope of this paper. There are indications that in Sr_2RuO_4 the low value of T_c , especially when compared with the cuprate high- T_c superconductors, is due to competition and near-cancellation between two different pairing symmetries [28]. It is to be expected, then, that changes in $\chi(\mathbf{q})$ would have drastic effects on T_c and coherence length ξ which should be visible as deviations from the universal Abrikosov-Gor'kov curve in the inset of Fig. 1. Within experimental errors, and for the doping range in which we were able to establish the superconducting properties, we see no such deviations. We therefore believe that our observations place significant constraints on the search for the mechanism of the superconductivity of Sr_2RuO_4 . In this context, it would also be interesting to directly measure the dynamical susceptibility of these samples, to gauge the extent to which the spin-fluctuation spectrum is changing as a function of \mathbf{q} .

In summary, we have studied the microscopic effects of doping La^{3+} for Sr^{2+} in the correlated electron metal Sr_2RuO_4 . An empirical, rigid-band shift, tight-binding parameterization of the electronic structure that incor-

porates constant many-body renormalizations allows a quantitative prediction of the evolution of both the Fermi surface geometry and the thermal properties of the doped material. Although this is not the first time that dHvA has been observed in the presence of doping in a correlated electron metal (a notable previous example is $\text{Ce}_{1-x}\text{La}_x\text{B}_6$ [29]), it is to our knowledge the first time that the rigid-band model has been put to such a sensitive test, especially for multi-band system. The superconducting properties remain remarkably unchanged in the face of a rapidly evolving, enhanced susceptibility spectrum, which raises intriguing questions about the mechanism of the unconventional superconductivity.

The authors thank A.J. Millis, T. Nomura, M. Braden, Kosaku Yamada, P. Monthoux, and G.G. Lonzarich for useful discussions. They also thank H. Fukazawa for technical supports and discussions, M. Yoshioka for technical supports, Y. Shibata and Takashi Suzuki for EPMA measurements at Hiroshima University. This work was in part supported by the Grant-in-Aid for Scientific Research (S) from the Japan Society for Promotion of Science (JSPS), by the Grant-in-Aid for Scientific Research on Priority Area 'Novel Quantum Phenomena in Transition Metal Oxides' from the Ministry of Education, Culture, Sports, Science and Technology, and by the Leverhulme Trust. One of the authors (N.K.) is supported by JSPS Postdoctoral Fellowships for Research Abroad, while S.A.G. gratefully acknowledges the support of the Royal Society.

-
- [1] Y. Maeno *et al.*, Nature **372**, 532 (1994).
 [2] T.M. Rice and M. Sigrist, J. Phys. Condens. Matter **7**, L643 (1995).
 [3] A.P. Mackenzie and Y. Maeno, Rev. Mod. Phys. **75**, 657 (2003).
 [4] A.P. Mackenzie *et al.*, Phys. Rev. Lett. **76**, 3786 (1996).
 [5] C. Bergemann *et al.*, Phys. Rev. Lett. **84**, 2662 (2000).
 [6] C. Bergemann *et al.*, Adv. Phys. **52**, 639 (2003).
 [7] T. Oguchi, Phys. Rev. B. **51**, 1385 (1995).
 [8] D.J. Singh, Phys. Rev. B. **52**, 1358 (1995).
 [9] A. Damascelli *et al.*, Phys. Rev. Lett. **85**, 5194 (2000).
 [10] Y. Sidis *et al.*, Phys. Rev. Lett. **83**, 3320 (1999).
 [11] M. Braden *et al.*, Phys. Rev. B. **66**, 064522 (2002).
 [12] I.I. Mazin and D.J. Singh, Phys. Rev. Lett. **79**, 733 (1997).
 [13] D.K. Morr P.F. Trautman, and M.J. Graf, Phys. Rev. Lett. **86**, 5978 (2001).
 [14] T. Nomura and K. Yamada, J. Phys. Soc. Jpn. **69**, 3678 (2000); *ibid.* **71**, 1993 (2002).
 [15] For instance, A. Damascelli, Z. Hussain, and Z.X. Shen, Rev. Mod. Phys. **75**, 473 (2003); J.M.D. Coey, M. Viret, and S.v. Molnar, Adv. Phys. **48**, 167 (1999).
 [16] M. Minakata and Y. Maeno, Phys. Rev. B **63**, 180504(R) (2001); K. Pucher *et al.*, Phys. Rev. B **65**, 104523 (2002).
 [17] M. Braden *et al.*, Phys. Rev. Lett. **88**, 197002 (2002).
 [18] N. Kikugawa and Y. Maeno, Phys. Rev. Lett. **89**, 117001 (2002).
 [19] K. Ishida *et al.*, Phys. Rev. B **67**, 214412 (2003).
 [20] N. Kikugawa, A.P. Mackenzie, and Y. Maeno, J. Phys. Soc. Jpn. **72**, 237 (2003).
 [21] S. Nakatsuji and Y. Maeno, Phys. Rev. Lett. **84**, 2666 (2000).
 [22] K. Hamacher, C. Gros, and W. Wenzel, Phys. Rev. Lett. **88**, 217203 (2002).
 [23] Z.Q. Mao, Y. Maeno, and H. Fukazawa, Mat. Res. Bull. **35**, 1813 (2000).
 [24] D. Shoenberg, *Magnetic Oscillations in Metals* (Cambridge University Press, Cambridge, 1976).
 [25] A.P. Mackenzie *et al.*, Phys. Rev. Lett. **80**, 161 (1998).
 [26] Z.Q. Mao, Y. Mori, and Y. Maeno, Phys. Rev. B. **60**, 610 (1999).
 [27] K. Ng and M. Sigrist, J. Phys. Soc. Jpn. **69**, 3764 (2000).
 [28] P. Monthoux and G.G. Lonzarich, private communication.
 [29] R.G. Goodrich *et al.*, Phys. Rev. Lett. **82**, 3669 (1999).